CANCER

# High-dose vitamin C enhances cancer immunotherapy

Alessandro Magrì[1,2]*, Giovanni Germano[1,2]*, Annalisa Lorenzato[1,2], Simona Lamba[2], Rosaria Chilà[1,3], Monica Montone[2], Vito Amodio[1,2], Tommaso Ceruti[4], Francesco Sassi[2], Sabrina Arena[1,2], Sergio Abrignani[5,6], Maurizio D'Incalci[4], Massimo Zucchetti[4], Federica Di Nicolantonio[1,2†], Alberto Bardelli[1,2†]



**Vitamin C (VitC) is known to directly impair cancer cell growth in preclinical models, but there is little clinical evidence on its antitumoral efficacy. In addition, whether and how VitC modulates anticancer immune responses is mostly unknown. Here, we show that a fully competent immune system is required to maximize the antiproliferative effect of VitC in breast, colorectal, melanoma, and pancreatic murine tumors. High-dose VitC modulates infiltration of the tumor microenvironment by cells of the immune system and delays cancer growth in a T cell–dependent manner. VitC not only enhances the cytotoxic activity of adoptively transferred CD8 T cells but also cooperates with immune checkpoint therapy (ICT) in several cancer types. Combination of VitC and ICT can be curative in models of mismatch repair–deficient tumors with high mutational burden. This work provides a rationale for clinical trials combining ICT with high doses of VitC.**

## INTRODUCTION

Checkpoint inhibitor–based immunotherapies that target cytotoxic T lymphocyte antigen 4 (CTLA-4) or the programmed cell death 1 (PD-1) pathways have achieved remarkable success in the treatment of selected malignancies. Immune checkpoint therapy (ICT) based on anti–PD-1/PD-L1 and/or anti–CTLA-4 antibodies elicits prominent and long-lasting responses in tumors with high mutational and neoantigen burdens such as a fraction of melanoma, urothelial, and lung cancers as well as mismatch repair–deficient (MMRd) or microsatellite instable (MSI) tumors (*1*–*6*). Unfortunately, even within tumors with high mutational and neoantigen burdens, only a subset of patients derives clinical benefit from ICT. For instance, approximately half of MMRd tumors do not respond to immune checkpoint modulators, and among those that respond, only a fraction achieve durable remissions (*3*, *7*, *8*). On the other hand, the clinical efficacy of immunotherapy remains very limited in extremely aggressive cancers (pancreatic) or in some of the most prevalent tumors, such as breast or microsatellite stable (MSS) colorectal cancer (*9*–*11*). In addition, in some cases, treatment-related adverse events limit ICT efficacy. For all the above reasons, there is a need to find safe combinatorial strategies that can boost the efficacy of ICT and expand the tumor types and number of patients who may benefit from cancer immunotherapy.

Vitamin C (VitC) is an essential dietary nutrient, and its chronic deficiency contributes to impaired immunity (*12*). Immune cells accumulate high intracellular concentrations of VitC, suggesting that this cofactor is crucial for the function of these cells (*12*, *13*). A possible effect of VitC on innate and adaptive immune responses in infectious diseases has been reported (*13*, *14*). It has also been shown that VitC can modulate gene expression and differentiation in lymphoid and myeloid cells (*15*–*17*). VitC can act as a cofactor of TET dioxygenases and histone demethylases that are involved in the DNA and histone demethylation reactions, thus modulating gene expression (*16*, *18*).

The anticancer effect of VitC has been investigated for decades with controversial results. Cameron and Pauling (*19*) first reported that concomitant intravenous and oral supplementation of VitC prolonged survival of terminal cancer patients treated with different regimens. These findings were not confirmed in subsequent controlled double-blind trials, in which oral administration of VitC did not elicit clinical benefit (*20*). Follow-up studies revealed that the route of administration strongly affects VitC pharmacokinetics, suggesting that this difference may underlie the discrepant results (*21*).

Recent studies have provided a better mechanistic understanding of potential VitC antitumoral effects. In addition to the epigenetic effect of VitC mediated by TET activity, recent works highlighted that high-dose VitC preferentially kills cancer cells in vitro and in mouse models by exerting pro-oxidant effects and disrupting iron metabolism (*22*, *23*). Some of these effects can be observed only when high-dose VitC is administered intravenously.

Despite extensive investigations, whether and how VitC modulates the tumor immune environment is mostly unknown, and the relevance of VitC as a cancer therapy remains unclear (*24*, *25*). While several clinical trials are exploring the efficacy of combining VitC with chemotherapy or targeted agents (*26*), the potential of combining VitC with immunomodulators for anticancer purposes has not been explored. In this study, we investigated whether VitC could modulate antitumor immune responses and cancer immunotherapy.

[1]Department of Oncology, University of Torino, 10060 Candiolo (TO), Italy. [2]Candiolo Cancer Institute, FPO-IRCCS, 10060 Candiolo (TO), Italy. [3]IFOM, The FIRC Institute of Molecular Oncology, 20139 Milan, Italy. [4]Department of Oncology, Istituto di Ricerche Farmacologiche Mario Negri IRCCS, 20156 Milan, Italy. [5]Istituto Nazionale Genetica Molecolare INGM 'Romeo ed Enrica Invernizzi', 20122 Milan, Italy. [6]Department of Clinical Sciences and Community Health, University of Milan, 20122 Milan, Italy.
*These authors contributed equally to this work.
†Corresponding author. Email: alberto.bardelli@unito.it (A.B.); federica.dinicolantonio@unito.it (F.D.N.)

## RESULTS

### VitC delays tumor growth in immunocompetent syngeneic mice

We asked whether VitC could exert anticancer effects not only in a cancer cell–autonomous manner but also through modulation of antitumor immune responses. To address this, we studied several mouse cancer models including colorectal (CT26 and MC38), breast (TS/A and 4T1), melanoma (B16-F10), and pancreatic (PDAC). To explore

the impact of the immune system on cancer growth, tumor volume was monitored in immunocompromised [nonobese diabetic–severe combined immunodeficient (NOD-SCID)] and immunocompetent syngeneic mice. Breast cancer cells were orthotopically injected in the mammary fat pad, whereas the other tumor cell lines were injected subcutaneously. Once the tumors reached around 100 $mm^3$ in volume (typically 5 to 10 days), immunocompetent (Fig. 1A) and immunocompromised animals (Fig. 1B) were randomized to receive either control vehicle or high-dose VitC (4 g/kg per day intraperitoneally). Contrary to humans, mice are capable of synthesizing VitC, and measurements of endogenous VitC in mice resulted in basal plasma concentrations within the range of 0.005 to 0.011 mM, which were unaffected by tumor presence. One hour after VitC dosing, its plasma concentrations raised nearly 1000-fold to over 5 mM (fig. S1). We observed that, in most cases, tumor growth was delayed by the addition of VitC only in the presence of a fully competent immune system (Fig. 1A).

A dose threshold effect of VitC was seen at daily doses including and above 1.5 g/kg intraperitoneally, whereas lower doses were unable to affect growth of TS/A orthotopic breast tumors in immunocompetent mice (fig. S2). The tumor antiproliferative effect of VitC was maintained in the presence of antioxidant *N*-acetyl cysteine (NAC) at an oral dose of 1.2 g/kg, which abrogated VitC pro-oxidative effects, as indicated by the staining of 8-oxoguanine as a sensor of oxidative stress–induced DNA damage (fig. S3, A and B). The evidence that VitC exerts maximal anticancer therapeutic effects in immunocompetent, but not immunocompromised, mice suggests that VitC antitumor activity is also dependent on some immunomodulatory functions and not only on its pro-oxidant effects.

## VitC affects tumor growth in a T cell–dependent manner

Immunocompromised NOD-SCID mice have impaired T and B lymphocyte development. T lymphocytes are the main effectors of tumor immune surveillance, and their modulation has therapeutic efficacy

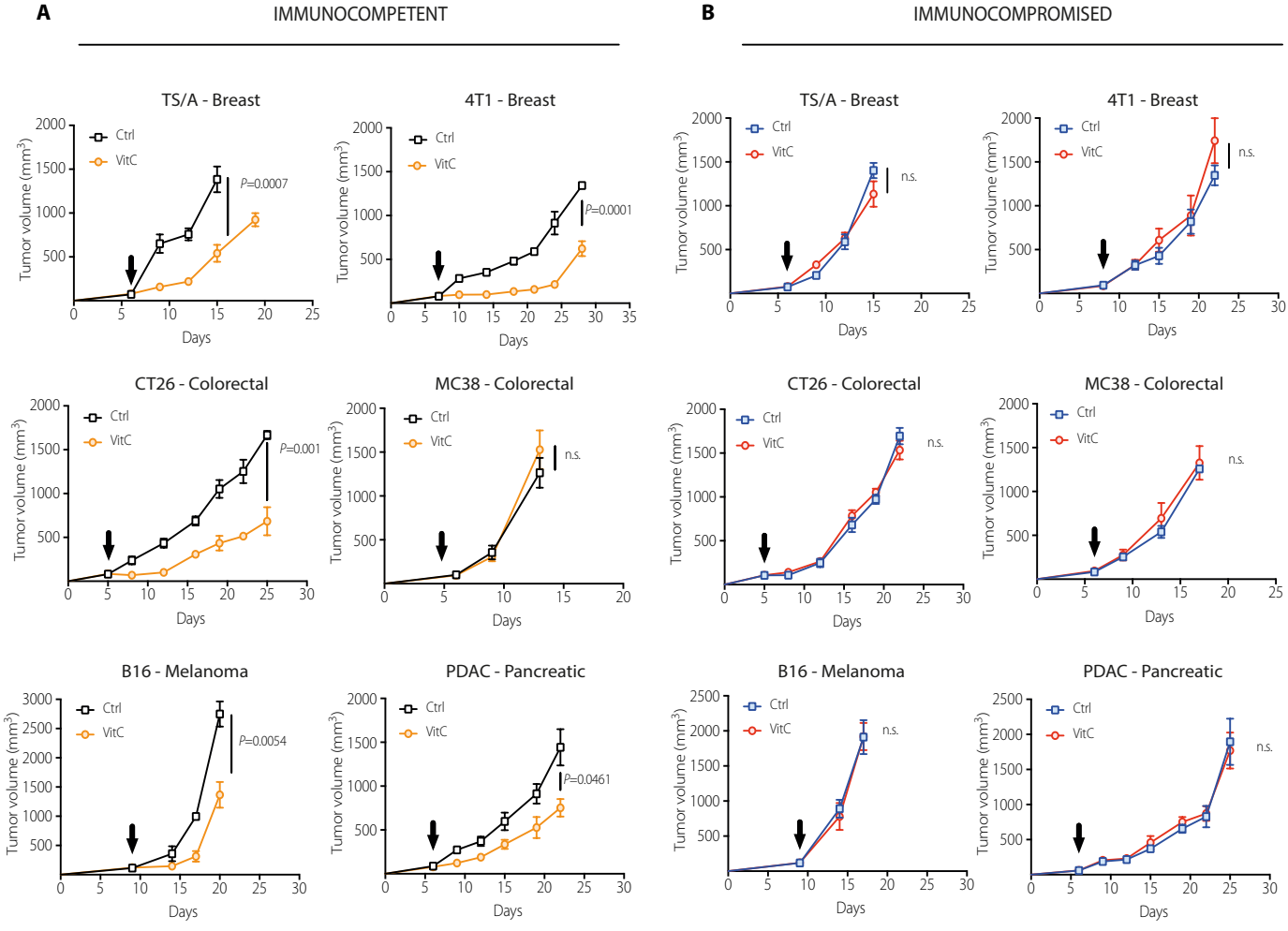


**Fig. 1. VitC delays tumor growth in immunocompetent syngeneic mice.** (**A**) The indicated cell lines were injected orthotopically (100,000 cells for TS/A and 4T1 models, 50% Matrigel) or subcutaneously (500,000 cells for CT26, MC38, B16, and PDAC models) in immunocompetent syngeneic mice. VitC (4 g/kg) was administered daily by intraperitoneal injections, and treatment was started when tumor volume reached around 100 $mm^3$ (indicated by the black arrow). (**B**) In parallel, mouse tumor cells were injected in immunocompromised NOD-SCID mice, and treatment was conducted in the same setting as indicated in (A). Every experimental group was composed at least of seven mice. Every experiment in (A) was performed at least twice. Data and error bars indicate mean ± SEM. *P* values were calculated by two-tailed unpaired Student's *t* test. n.s., not significantly different; Ctrl, control.

(*27*). We found that T lymphocytes isolated from the spleen of VitC-treated immunocompetent animals, when activated in vitro, produced higher interferon-γ (IFN-γ) concentrations in comparison with control mice (Fig. 2, A and B; see representative flow cytometry plots in fig. S4), suggesting that these lymphocytes may contribute to VitC immunomodulation.

Thus, to address the impact of T lymphocytes in the anticancer effects of VitC, we used two different approaches. On the one hand, we repeated the experiment shown in Fig. 1A in the presence of monoclonal antibodies (mAbs) targeting CD4- or CD8-positive T cells. An isotype antibody served as a control. We observed that anti-CD4 or anti-CD8 antibodies abolished the anticancer effect of VitC in breast TS/A and colorectal CT26 tumors (Fig. 2, C and D).

On the other hand, we adoptively transferred T lymphocytes from immunocompetent to immunocompromised animals. To this purpose, we first injected breast cancer cells (TS/A) in the mammary fat pad of syngeneic mice and, when tumors reached at least 100 $mm^3$ in volume, treated the mice with VitC or control vehicle (Fig. 2E). After 30 days, spleens were explanted, and CD4 and CD8 T cells were isolated (*28*). In parallel, TS/A cells were implanted in immunocompromised mice. Five and 10 days after TS/A cell implantation, CD4 and CD8 T cells isolated from VitC- or control vehicle–treated immunocompetent mice were injected intravenously into immunocompromised animals (see representative flow cytometry plots of isolated cells in fig. S5). Adoptive transfer of CD4 T cells showed antitumor activity irrespective of previous VitC treatment (Fig. 2F), whereas adoptive transfer of CD8 T cells was able to impair tumor growth only when lymphocytes were isolated from VitC-treated animals (Fig. 2G). Because it is known that CD4 T cells can regulate CD8 T cells, we hypothesized that CD4 T cells could be required to costimulate CD8 T cells in the presence of VitC. To test this hypothesis, we repeated the experiment shown in Fig. 2G by first depleting CD4 T cells in immunocompetent mice, in which we then orthotopically inoculated breast TS/A cells. Once tumors engrafted, mice were treated with VitC and the isotype control antibody (fig. S6). Thirty days after cell injection, spleens were collected and CD8 T cells from vehicle- or VitC-treated mice that had been depleted of CD4 T cells, as well as from animals pretreated with the isotype control antibody, were transferred into immunocompromised NOD-SCID animals bearing TS/A orthotopic tumors. Consistent with results shown in Fig. 2G, CD8 T cells impaired tumor growth only when transferred from VitC-treated animals and not from isotype control mice. However, adoptive transfer of CD8 T cells from VitC-treated donor mice that had been concomitantly depleted of CD4 T cells did not induce antitumor activity in immunocompromised mice (Fig. 2H). Together, these results show that treatment with high-dose VitC delays tumor growth and suggest that this effect depends on T lymphocytes, primarily on CD8 T cells. They also suggest that the presence of CD4 T cells is required to engage the cytotoxic potential of CD8 T cells in VitC-treated model systems.

### VitC enhances the efficacy of ICT

ICT can unleash the immune system and induce prolonged remissions in several tumors, but its efficacy is still very limited in some of the most prevalent malignancies such as breast and colon cancer (*27*, *29*, *30*). Intrigued by the finding that the antitumor activity of VitC was dependent on T cells, we assessed whether VitC could enhance the efficacy of ICT. Immune checkpoint modulators (anti–PD-1 and anti–CTLA-4 mAbs, ICT) alone and in combination were administered to mice bearing syngeneic pancreatic, breast, or colorectal tumors. In pancreatic PDAC and breast 4T1 models, the triple therapy combining VitC with anti–PD-1 and anti–CTLA-4 (VitC + ICT) induced tumor growth impairment compared to single treatments, but without eradicating the tumors (Fig. 3, A and B, and fig. S7). In the second breast cancer model (TS/A), combinatorial VitC + ICT induced prolonged tumor growth impairment (Fig. 3C). A subset of mice (8 of 13) that received the triple therapy rejected TS/A tumors and remained tumor-free for up to a year and eventually died without evidence of cancer, suggesting that the treatment had been curative (Fig. 3D and fig. S8A). In the subset of mice that displayed complete regression, no tumors developed even when they were later rechallenged with the same cancer cells (Fig. 3D), indicating that mice developed complete immune responses and that effective antitumor memory T cells had been expanded.

Treatment with VitC and immunomodulators in the previous experiments were administered when tumors were approximately 100 $mm^3$ in volume. As previously reported by another group (*31*), CT26 tumors show relatively high mutational burden and are responsive to dual combinatorial CTLA-4 and PD-1 blockade when treatment is administered to animals bearing tumors between 400 and 600 $mm^3$ in volume. To study the impact of combined VitC and ICT on the CT26 colon cancer model, we treated tumors of around 1000 $mm^3$ in volume that are refractory to ICT. Despite the marked disease burden, the triple therapy induced strong tumor impairment and remission in several animals (7 of 13) (Fig. 3E). The subset of mice experiencing a complete response remained tumor-free up to a year, and no tumor developed even when they were later rechallenged with the same cancer cells, indicating effective antitumor immune memory (Fig. 3F and fig. S8B).

### The addition of VitC to ICT enhances recruitment of T lymphocytes in the tumor microenvironment

In support of the immunomodulatory functions of VitC, immunofluorescence analysis of TS/A breast tumors showed that VitC treatment induced tumor infiltration by both CD4 and CD8 T lymphocytes, which were further increased by combining VitC and ICT (Fig. 4, A and B).

To further characterize the immunological response observed after combining VitC and ICT, we explanted orthotopically grown TS/A breast tumors and isolated infiltrating immune cell fractions from control and treated mice. Flow cytometry analysis revealed that neither the CD45-positive nor the T regulatory cell fractions were modulated in tumors treated with VitC alone (fig. S9). Combined treatment with VitC and ICT induced activation of tumor-infiltrating lymphocytes, as shown by positive staining for the T cell activation marker CD69 and the effector/memory CD44 marker on CD4 and CD8 T lymphocytes (Fig. 4, C and D; see representative flow cytometry plots in figs. S10 and S11).

### Addition of VitC induces complete remission of MMRd tumors unresponsive to single immune checkpoint inhibitors

ICT is approved for the treatment of any tumor type displaying microsatellite instability, which is the result of MMR inactivation. Unfortunately, only a subset of MMRd tumors respond to immune checkpoint modulators, and among those that respond, only a fraction derive long-lasting benefits (*3*, *7*, *8*). We wondered whether VitC could improve the magnitude and durability of clinical benefit from

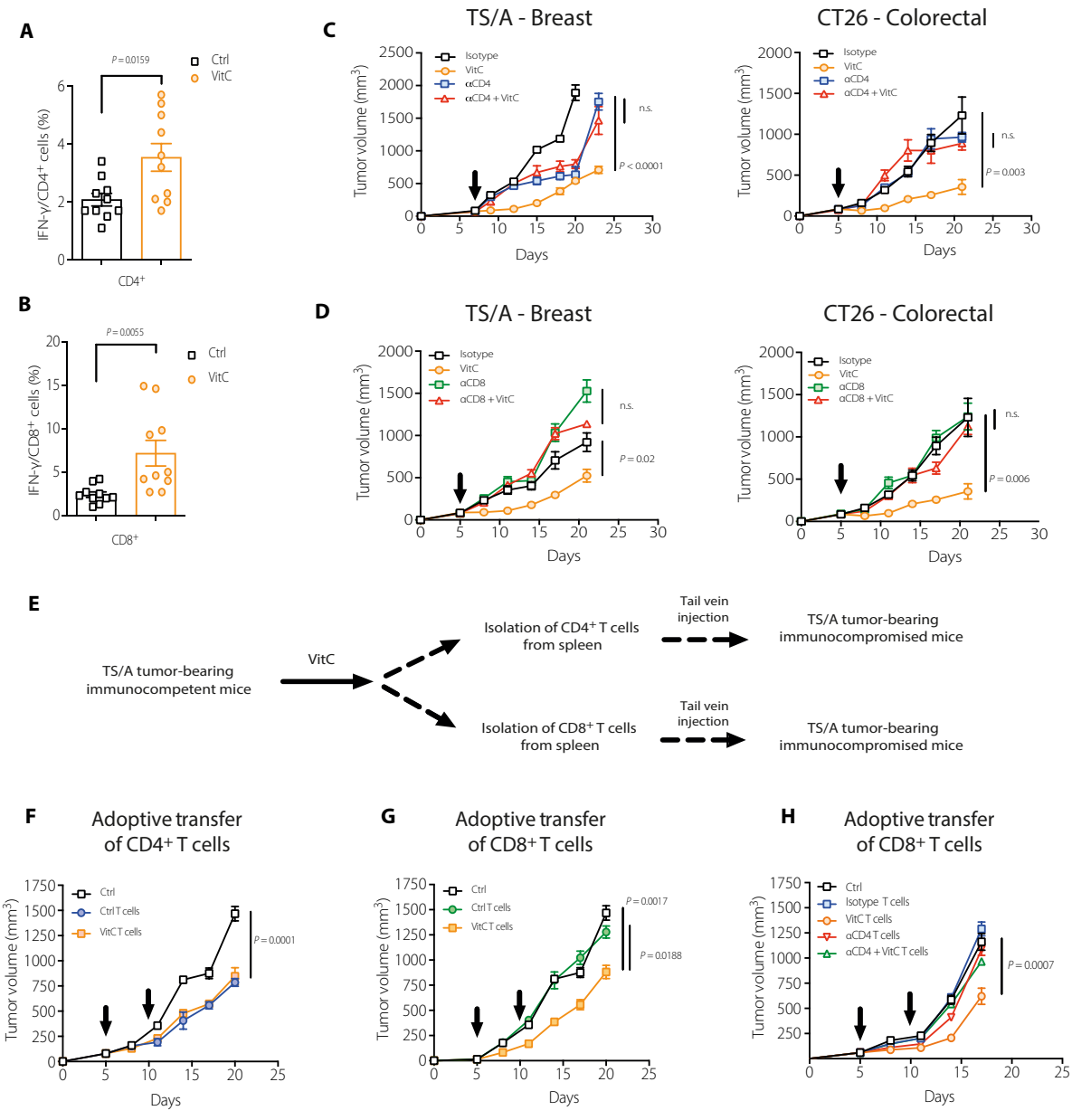


**Fig. 2. VitC affects tumor growth in a T cell–dependent manner.** (**A** and **B**) Flow cytometry analysis of IFN-γ release on CD4 (A) and CD8 (B) spleen-derived lymphocytes isolated from untreated and VitC-treated mice injected orthotopically with TS/A cancer cells. Spleens were harvested 30 days after tumor cell injection, and T lymphocytes were stimulated in vitro. Percentages were calculated relative to CD4 and CD8 live events. The indicated cell percentages were gated on $CD45^+$ live, $CD4^+/CD8^+$, and IFN-γ (500,000 events were taken for each sample). (**C**) Depletion of CD4 T cells and (**D**) depletion of CD8 T cells in the indicated cell models. Mice were treated with anti-CD4 (αCD4)– or anti-CD8 (αCD8)–depleting mAbs (400 μg per mouse at day 0 and then 100 μg per mouse at day 1, day 2, and every 3 days through the entire course of the experiment). Control mice were administered the isotype antibody. (**E**) Adoptive T cell transfer was performed according to the indicated experimental design. (**F** and **G**) Adoptive cell transfer of untreated and VitC-treated CD4 T cells (F) or CD8 T cells (G) isolated from the spleens of immunocompetent mice and infused into NOD-SCID mice orthotopically injected with TS/A; CTRL indicates tumor growth in NOD-SCID without T cell administration. (**H**) To test the effect of VitC on CD8 T cells in the absence of CD4 lymphocytes, immunocompetent mice were pretreated with a depleting CD4 T cell antibody or isotype antibody (as a control) and then administered VitC. CD8 T cells isolated from these immunocompetent mice were injected into the tail vein of immunocompromised NOD-SCID mice bearing orthotopic TS/A tumors ($n = 4$). Black arrows indicate the time points of T cell tail vein infusion. Five million T cells per injection were administered to each mouse. Every experimental group was composed of at least of six mice, with the exception of adoptive cell transfer experiments, which were composed of four mice per group. Every experiment was performed at least twice except for those shown in (A), (B), (D), and (H). Data and error bars indicate mean ± SEM. *P* values were calculated using two-tailed unpaired Student's *t* test for (A) and (B); one-way analysis of variance (ANOVA) for all other panels at the indicated time points.

immune therapies on MSI tumors. To this end, we used MMRd tumor models that we had previously developed by genetic inactivation of Mlh1 in colorectal and breast cancer murine cells (*32*). Mlh1 knockout (MLH1-KO) cells have increased mutational burden, augmented number of predicted neoantigens, and higher immunogenicity (*32*). Because we previously found that MLH1-KO cells grow

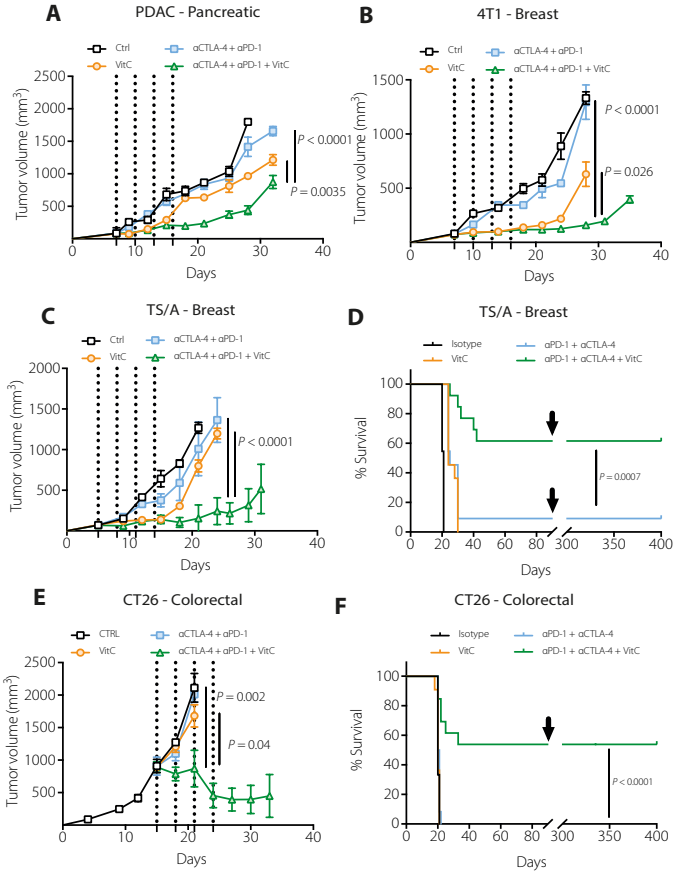


**Fig. 3. The efficacy of ICT is enhanced by VitC.** (**A**) PDAC pancreatic cancer cells were injected subcutaneously (500,000 cells) into syngeneic mice that were treated with VitC, ICT, or their combination. (**B**) 4T1 breast cancer cells were injected orthotopically (100,000 cells, 50% Matrigel) in syngeneic mice that were treated with VitC, ICT, or their combination. (**C**) TS/A breast cancer cells were injected orthotopically (100,000 cells, 50% Matrigel) in syngeneic mice that were treated with VitC, ICT, or their combination. (**D**) Tumor relapse-free survival of mice treated with VitC, ICT, or their combination and followed for over a year. Two independent experiments performed on a total of $n = 13$ mice are shown in survival curves. The vertical black arrows indicate the time point at which mice were rechallenged with live tumor cells. (**E**) CT26 colorectal cancer cells were injected subcutaneously (500,000 cells) in syngeneic mice. (**F**) Tumor relapse-free survival of mice treated with VitC, ICT, or their combination and followed up to a year. Two independent experiments performed on a total of $n = 13$ mice are shown in survival curves. The vertical black arrow indicates the time point at which mice were rechallenged with live tumor cells. VitC (4 g/kg) was administered intraperitoneally 5 days per week starting when tumors reached a volume around 100 $mm^3$ in the TS/A, 4T1, and PDAC models. VitC treatment started when tumor volume was around 800 to 1000 $mm^3$ in the CT26 model. Anti–CTLA-4 (200 μg per mouse) and anti–PD-1 (250 μg per mouse) were given at the time points indicated by the dashed vertical lines in the graphs. In combinatorial treatments, VitC was administered starting with the first cycle of immunotherapy. Every experimental group was composed of at least five mice. Every experiment was performed twice except for those shown in (A) and (B). Data and error bars indicate mean ± SEM. Statistical analysis used one-way ANOVA for tumor growth comparison at the indicated time points and log-rank test (Mantel-Cox) for survival analysis.

slower than their parental counterpart in syngeneic mice (*32*), we initially injected them into immunocompromised animals until large tumors were established. Next, tumor samples were explanted, fragmented, and transplanted into multiple immunocompetent mice that were then randomized to receive either control vehicle or VitC, as shown in Fig. 5A. In parallel, matched Mlh1 wild-type (MLH1-WT) and MLH1-KO colorectal and breast tumors were also treated with VitC in immunocompromised animals. Once again, independently of the MLH1 status (and neoantigen burdens), VitC had no effect on tumor growth in immunocompromised mice (fig. S12). In immunocompetent hosts, the growth of MMRd was slower compared with MMR-proficient tumors, as expected (Fig. 5, B and C) (*32*). Notably, the effect of VitC alone was much more prominent in MMRd cancers than in their MMR-proficient counterparts (Fig. 5, B and C). These findings suggest that the antitumor effect of VitC is enhanced in mice with tumors harboring increased mutational/neoantigen burdens. The addition of individual immunomodulators (anti–PD-1 or anti–CTLA-4) to VitC improved anticancer responses in mice bearing sizeable MMRd tumors (Fig. 5D and figs. S13 and S14). The combination of VitC with anti–CTLA-4 induced complete tumor regression in most mice (fig. S13), and no relapses were seen for up to a year (Fig. 5E). Notably, after about 1 month of treatment, the effect of VitC and anti–CTLA-4 was comparable to the effect induced by the combination of anti–PD-1 and anti–CTLA-4 mAbs (Fig. 5D). Last, no tumors developed when mice bearing MMRd tumors that achieved complete response on VitC and ICT combination were later rechallenged with the same cancer cells (Fig. 5E). This indicates that these mice had developed protective immunity and immunological memory. Autoimmune reactions can be observed in animals treated with CTLA-4 inhibitors as a consequence of T regulatory cell depletion. Illness, chronic inflammation of ears and eyelids, and reduced motility have been observed during chronic T regulatory cell depletion in mice (*33*). We found that treatments were generally well tolerated, and no signs of autoimmune reactions were recorded in any of the treatment arms.

## DISCUSSION

In this work, we investigated whether and to what extent the anticancer activity of VitC relies on the host immune system. We found that in most murine cancer models tested, VitC potentiates adaptive immune responses against cancer cells and can effectively combine with ICT. These effects are therapeutically relevant in MMR-proficient tumors, and the addition of VitC to ICT is often curative in MMRd tumors.

Several studies have previously shown that administration of VitC can impair or delay tumor development in mice (*22*, *23*, *26*, *34*, *35*). While the different anticancer efficacy of VitC in immunocompromised versus immunocompetent animals has been previously reported for the B16-F10 melanoma model (*36*), the extent and the relevance of a fully competent immune system have not been systematically explored. Our study shows that VitC can delay tumor growth by stimulating adaptive immune responses in several murine cancer models. We acknowledge that VitC immunomodulatory effects are not expected to be universal, because at least one model, namely, MC38 colorectal tumors, proved to be refractory. Future work should focus on understanding the mechanisms underlying the lack of VitC efficacy in these outlier tumors. We also note that clinical trials in cancer patients have shown no clear benefit from high-dose VitC in monotherapy (*26*), whereas our data indicate that VitC alone delays the growth of relatively small tumors in the presence of a competent immune system in mice. Hence, caution should be taken when translating findings from model systems to humans.

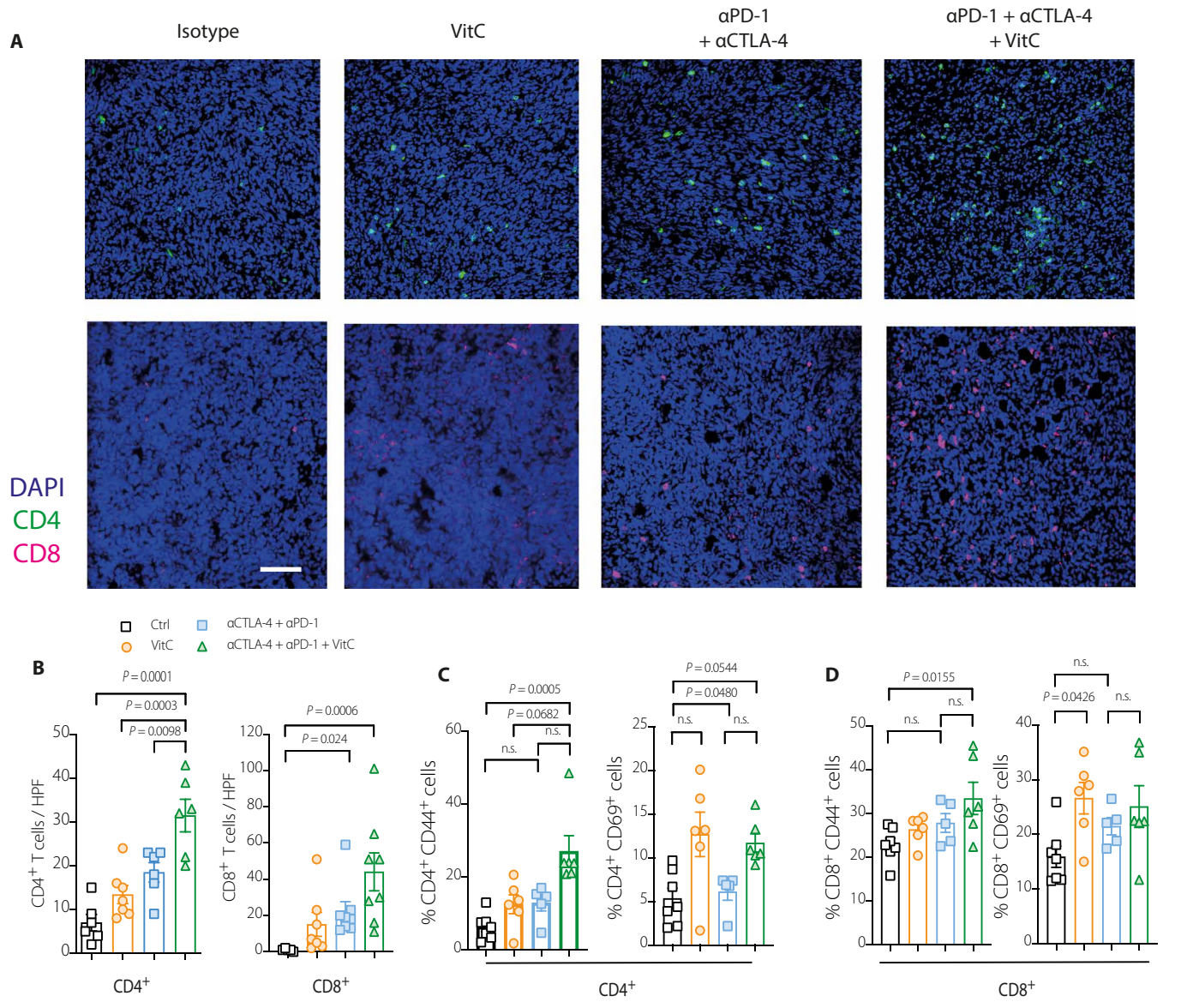


**Fig. 4. VitC in combination with ICT enhances infiltration and activation of T lymphocytes.** TS/A orthotopic tumors were explanted and analyzed for immune infiltration. (**A**) Immunofluorescence analysis of CD4 and CD8 tumor-infiltrating lymphocytes. Maximum projection of a 10-image stack along the *z* axis. Scale bar is representative of 75 μm. (**B**) Quantification of CD4 and CD8 T cells from (A). T cell counts per high-power field (HPF) from six different mice. (**C** and **D**) TS/A orthotopic tumors were explanted, single cell–suspended, and analyzed by flow cytometry. Staining for memory/effector markers on CD4 (C) and CD8 (D) T cells. The fraction of positive cells was calculated on $CD4^+$ and $CD8^+$ live events, respectively (500,000 events were acquired for each sample). Individual values are presented, and error bars indicate ±SD. *P* values were calculated using nonparametric analysis for (B) and (C); one-way ANOVA for (D).

We show that ablation of CD8 T lymphocytes in immunocompetent mice severely impairs and often completely abolishes VitC effects. Our results also hint at a critical role of CD4 T cells to modulate CD8 T cells in the presence of VitC. VitC has previously been shown to enhance differentiation and proliferation of myeloid and lymphoid cells, likely due to its gene-regulating effects (*15*, *16*). Physiological concentrations of VitC were reported to preserve the immunosuppressive capacity of T regulatory cells and prevent autoimmunity (*15*, *37*). We found that high doses of VitC did not affect the percentage of tumor-infiltrating T regulatory cells. Our study shows that in vivo administration of VitC increases the number of tumor-infiltrating T cells and enhances activation of CD4 and CD8 effector T cells. This is in agreement with a recent study that also showed increased intratumoral T cell infiltration when mice were treated with VitC (*35*). Our findings are also in line with another study that found a higher frequency of CD8 effector and memory T cells when mice were inoculated with tumor lysate–loaded dendritic cells that had been pretreated ex vivo with VitC (*38*).

In this work, we did not investigate the molecular mechanisms leading to T cell activation after administration of VitC in mice, because this aspect has already been studied. Several studies have previously shown that VitC leads to epigenetic modulation of T cells and their activation, by acting as a cofactor for both DNA and histone demethylases (*18*, *39*). In relation to this, we speculate that VitC

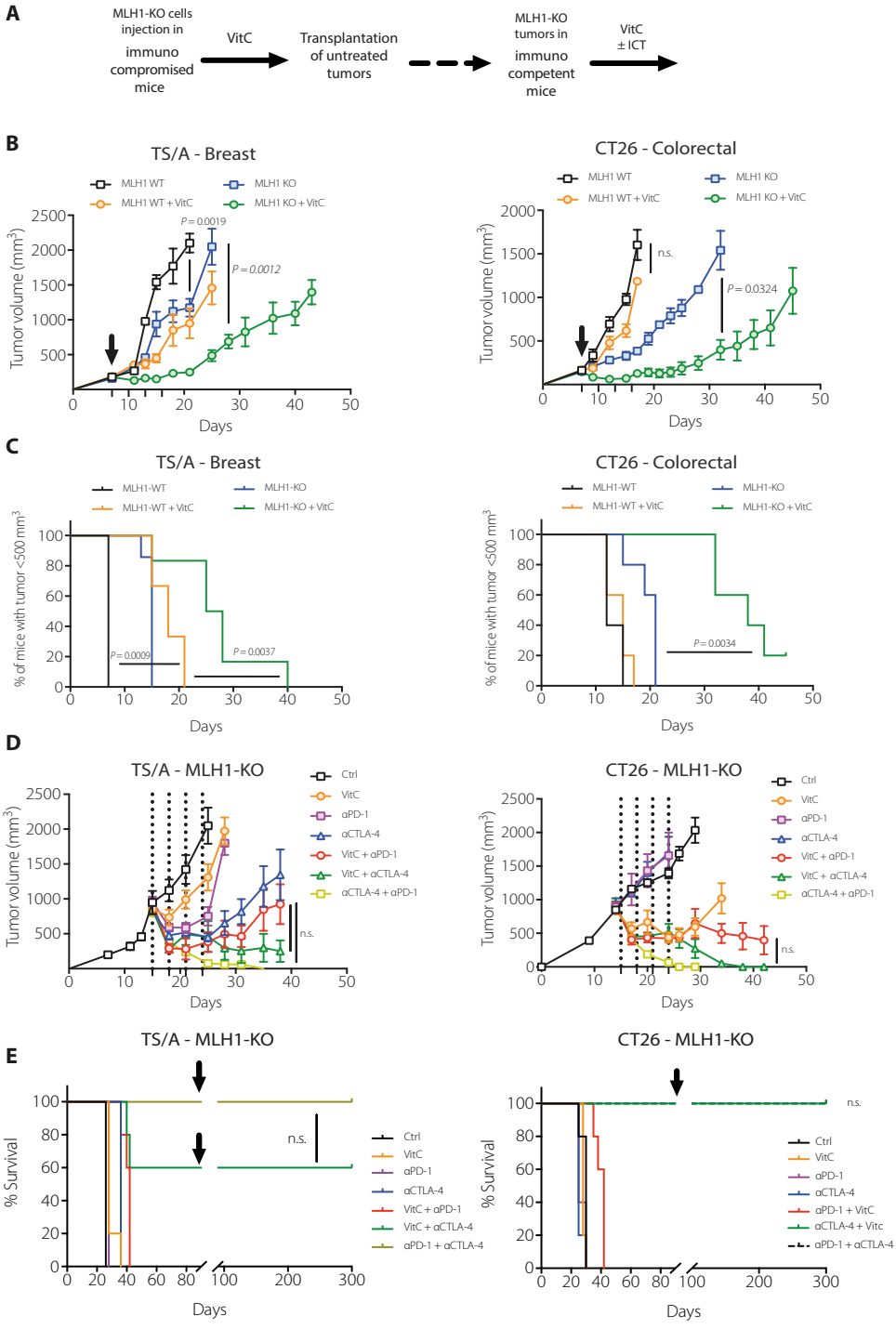


**Fig. 5. Addition of VitC to individual immune checkpoint inhibitors induces remission in MMRd tumors.** (**A**) MLH1-WT and MLH1-KO cells were first subcutaneously injected (500,000 cells) in immunocompromised mice (shown in fig. S12) according to the indicated experimental design. (**B**) Small fragments of untreated tumors bearing the indicated MLH1 genotype were transplanted into immunocompetent syngeneic mice; VitC (4 g/kg) was administered by intraperitoneal injection 5 days per week, starting when tumors reached a volume around 150 to 200 $mm^3$ (black arrow) to ensure tumor engraftment. (**C**) Percentage of mice [animals from the experiment shown in (A)] whose tumor volume was less than 500 $mm^3$, which we set as an arbitrary end point. (**D**) In the same setting as in (A), MLH1-KO tumors were transplanted into immunocompetent syngeneic mice and treated with ICT and VitC (4 g/kg) starting at a tumor volume of 800 to 1000 $mm^3$. Anti–CTLA-4 (200 μg per mouse) and anti–PD-1 (250 μg per mouse) were given at the time points indicated by the dashed vertical lines in the graphs. (**E**) Tumor relapse-free survival of mice treated with VitC, immune checkpoint inhibitors, or their combination shown in (C). The black arrows indicate tumor rechallenge with the same cancer cells. Every experimental group was composed of at least five mice. Every experiment was performed twice except for the models shown in (B) and (C). Data and error bars indicate mean ± SEM. Statistical analysis used two-tailed unpaired Student's *t* test for (B); one-way ANOVA for (D) at the indicated time points. Survival analysis in (C) and (E) used log-rank test (Mantel-Cox) analysis.

may cause rejuvenation of T cells, favoring their expansion and clonal diversity (*40*). Follow-up studies to delve into the underlying mechanism of the observed therapeutic effect of VitC in the model systems described in this work are warranted.

In addition to promoting DNA demethylation mediated by TET enzyme activation, high doses of VitC may kill cancer cells via oxidative stress and by disrupting iron metabolism (*22*). However, we found that concomitant administration of a reactive oxygen species (ROS) scavenger did not blunt VitC efficacy in immunocompetent mice, indicating that oxidative stress is unlikely to exert a major impact in the models and experimental settings described in this work. Nevertheless, previous reports have shown that high doses VitC can inhibit the growth of human tumors inoculated in immunocompromised mouse models (*23*, *26*). Together, these previous works and the data reported in our study suggest that there are multiple means by which VitC exerts its antitumor effects, and the immune-mediated mechanism might be independent of, and in addition to, the pro-oxidative mechanism.

We report that the addition of VitC can potentiate the efficacy of combined anti–CTLA-4 and anti–PD-1 blockade in breast, pancreatic, and colorectal MMR-proficient murine models. Not only did this combination delay tumor growth in most cases, but also in a few mice, complete regressions were observed. We found that combining VitC and ICT further enhanced tumor-infiltrating CD8 T cells compared to the increase observed with single treatments.

Immune checkpoint inhibitors are approved for the treatment of several malignancies. However, intrinsic unresponsiveness is seen

in most cases. For instance, only a fraction of patients with MMRd tumors benefit from immunotherapy. Combinations of immune checkpoint inhibitors including anti–CTLA-4 and anti–PD-1 achieve responses in a larger fraction of MMRd patients, but at the price of higher toxicities (*41*). Although addition of VitC did not improve the activity of anti–PD-1 alone, VitC strongly enhanced the efficacy of anti–CTLA-4 as a monotherapy, and their combination induced a complete response in several mice bearing MMRd tumors. In relation to this, a dose reduction of ICT might be explored in combinatorial regimens with VitC to mitigate toxicity or adverse events induced by immunotherapy.

The mechanism underlying the cooperation between VitC and immune checkpoint inhibitors deserves further studies. We found increased production of IFN-γ by T cells extracted after VitC administration. This is consistent with the notion that VitC can modulate cytokine generation (*13*), although we acknowledge that we did not investigate this aspect in detail. It is possible that VitC improves T cell responses and tumor control during treatment with immune checkpoint inhibitors by reverting T cell exhaustion–associated DNA methylation programs (*40*). Together, this evidence prompts us to speculate that VitC pleiotropic functions can revert a growth-permissive tumor immune environment.

We do not rule out that VitC could exert its functions not only on immune cells but also on cancer cells. In this regard, a recent study has shown that VitC can stimulate TET2 activity in cancer cells and potentiate the efficacy of anti–PD-L1 or anti–PD-1 immune therapy in mouse melanoma cells ectopically expressing the ovalbumin antigen or a lymphoma model, respectively (*35*, *42*).

The evidence that a vitamin has such a marked impact on ICT in highly aggressive mouse cancer models prompted us to consider designing clinical trials, which must keep in mind the points highlighted below. Patients with advanced cancer reportedly have compromised VitC status, and intravenous administration of VitC would likely be required to achieve pharmacologically relevant concentrations (*21*). Although the highest dose of VitC typically given to humans is lower than that used in murine experiments, ascorbic acid concentrations in plasma can peak at 10 to 20 mM in cancer patients after intravenous administration (*43*), which is in the same range or possibly higher than what we found in rodents treated with high-dose intraperitoneal VitC. Nevertheless, we have not measured plasma VitC concentrations when it was given with ICT in mice, so we cannot rule out that drug-drug interactions could have influenced VitC pharmacokinetics in combinatorial regimens. On the bright side, VitC is known to be well tolerated at high doses, and intravenous administration is generally considered to be safe. However, the optimal dose or duration of VitC treatment has not been established (*26*). This is particularly relevant when planning combination studies with immune checkpoint inhibitors that are often administered for several months or years. Results from the adoptive cell transfer experiments suggest that VitC exposure could be critical in the priming and/or clonal expansion phases as well as during lymphocyte-mediated cancer cell killing. On the basis of our findings, we propose that VitC should be tested concomitantly with the first few cycles of immune checkpoint inhibitors. Although mice received only four cycles of ICT, no signs of immune-related adverse events or other toxicities were seen in animals treated with VitC and ICT, suggesting that combinatorial regimens may be tolerated by cancer patients (*33*). Nevertheless, this issue will require assessment in clinical studies in which escalating doses of VitC should be administered with concomitant ICT. VitC has been shown to decrease chemotherapy-related toxicities in cancer patients (*26*, *44*); the same effect might occur in the presence of ICT, and further work in this direction is warranted. In summary, we describe that VitC can stimulate anticancer adaptive immunity and enhance the efficacy of immune checkpoint inhibitors in mouse cancer models, including MMR-proficient and MMRd tumors, thus paving the way for the design of combination clinical trials testing VitC-mediated immunomodulation.

## MATERIALS AND METHODS

### Study design

The objectives of this study were to assess whether high-dose VitC might exert anticancer activity through the immune system and to verify whether combinatorial treatment with ICT might limit tumor growth in mouse preclinical cancer models. The evidence that a fully competent immune system maximizes the anticancer effects of VitC was demonstrated by administering VitC to immunocompetent and immunocompromised tumor-bearing mice in parallel. We also showed that CD4 and CD8 T cells are the main mediators of the anticancer activity induced by VitC. We demonstrated this by directly depleting the CD4 and CD8 T lymphocytes in immunocompetent mice by administering specific depleting antibodies. The helper and cytotoxic roles of CD4 and CD8 T cells were verified by adoptive transfer experiments of lymphocytes from immunocompetent to immunocompromised mice. The cooperation of high-dose VitC and ICT was demonstrated by administering combinatorial treatments to mice bearing MMR-proficient and MMRd mouse tumors. Immunofluorescence analyses were performed to uncover that the addition of VitC to ICT increases the infiltration of CD4 and CD8 T lymphocytes. In all experiments, control and experimental treatments were randomly administered to age- and sex-matched mice. Tumor burden was monitored over time to assay responses to specific treatments and combinations. Animals were examined for toxicity by periodic observation, and samples were collected. Blinding was not used in this study. However, measurements of tumors were taken before the identification of the cages. The numbers of experimental replicates are indicated in the figure legends. Sample sizes were chosen empirically to ensure adequate statistical power and were in line with the standards for the techniques used in the study.

### Mouse cell lines

The TS/A breast cancer cell line was established from a moderately differentiated mammary adenocarcinoma that arose spontaneously in a Balb/c mouse (*45*). TS/A cells were provided by F. Cavallo (Molecular Biotechnology Center, University of Torino). CT26 is a mouse undifferentiated colon carcinoma, derived from Balb/c mice (*46*). CT26 cells were purchased from the American Type Culture Collection (ATCC). MC38 is a mouse colon adenocarcinoma line derived from a C57/BL6 mouse, and cells were provided by M. Rescigno (European Institute of Oncology). 4T1 is a spontaneous mammary adenocarcinoma derived from a Balb/c mouse and was purchased from ATCC (*47*). PDAC cells were isolated from FVB transgenic mice bearing pancreatic cancers with the following genotype: $p48^{cre}$, $Kras^{LSL\text{-}G12D}$, $p53^{R172H/+}$, and $Ink4a/Arf^{flox/+}$. PDAC cells were provided by D. Hanahan (*48*) (ISREC, EPFL, Lausanne). B16-F10 is a melanoma cell line derived from a C57/BL6 mouse, purchased from ATCC (*49*). CT26, MC38, 4T1, and PDAC cells were cultured in RPMI

1640–10% fetal bovine serum (FBS) plus 2 mM glutamine, penicillin (100 IU/ml), and streptomycin (100 μg/ml; Sigma-Aldrich). TS/A and B16-F10 cells were cultured in Dulbecco's modified Eagle's medium (DMEM)–10% FBS plus 2 mM glutamine, penicillin (100 IU/ml), and streptomycin (100 μg/ml; Sigma-Aldrich). All cell lines were tested for mycoplasma regularly. To ensure that the parental cell models were tumorigenic, before starting the experiments, all the lines were injected into matched syngeneic mice. On tumor formation, we re-established in vitro cell cultures.

### Animal studies

All animal procedures were approved by the Ethical Commission of the Candiolo Cancer Institute and by the Italian Ministry of Health, and they were performed in accordance with institutional guidelines and international law and policies. The number of mice included in the experiments and the inclusion/exclusion criteria were based on institutional guidelines. We observed tumor size limits (maximum allowable diameter of 20 mm) in accordance with institutional guidelines. Six- to 8-week-old female and male C57BL/6J, Balb/c, FVB, and NOD-SCID mice were used according to the approved protocol. Mice were obtained from Charles River. All experiments involved a minimum of five mice per group. Tumor size was measured every 4 days and calculated using the formula $V = (d2 \times D)/2$ ($d$ = minor tumor axis; $D$ = major tumor axis) and reported as tumor volume ($mm^3$; mean ± SEM of individual tumor volumes). Animals were kept under supervision by veterinary personnel throughout the entire duration of the experiments. Mice were checked at least three times a week for signs of illness, inflammation of ears and eyelids, and reduced motility, because these side effects had been previously reported for animals treated with CTLA-4–targeted mAbs (*34*). The investigators were not blinded; measurements were acquired before the identification of the cages. No statistical methods were used to predetermine sample size.

### Mouse treatments

Ascorbate (Sigma-Aldrich) was prepared weekly by resuspending the powder in sterile water. Ascorbate was administered intraperitoneally 5 days per week at a dosage of 4 g/kg. The anti-mouse PD-1 (clone RMP1-14), anti-mouse CTLA-4 (clone 9H10), anti-mouse CD4 (YTS191), anti-mouse CD8a (YTS169.4), rat IgG2a, and polyclonal Syrian hamster immunoglobulin G (IgG) and rat IgG2b antibodies were purchased from BioXcell. Randomization was used for the experiments in which therapeutic effects had to be evaluated. Animals were treated intraperitoneally with 250 μg of anti–PD-1 antibody per mouse and 200 μg of anti–CTLA-4 antibody per mouse. Treatments were administered at the time points indicated in the graphs after checking for tumor establishment. In combinatorial treatments, VitC was administered starting with the first cycle of immunotherapy. Isotype controls were injected according to the same schedule. Anti-mouse CD4 and CD8a were used for depletion of T cells in immunocompetent mice. Anti-mouse CD4, CD8a, and matched isotype mAbs (400 μg per mouse) were injected intraperitoneally on the day of tumor inoculation. Depleting antibodies were administered (100 μg per mouse) on days 1 and 2 and then every 3 days since tumor cell injection. Depleting antibodies and matched isotypes were administered every 3 days throughout the course of the experiments. Flow cytometry analysis was performed every 3 days to assess the numbers of $CD4^+$ and $CD8^+$ cells in the bloodstream of mice. The fraction of $CD4^+$ or $CD8^+$ cells relative to $CD45^+$ cells was around 20% before and 0.5% after the administration of depleting antibody. The low fraction of $CD4^+$ and $CD8^+$ cells (0.5%) was maintained throughout the entire experiment.

### Flow cytometry cell analysis

Mouse tumors were cut into small pieces, disaggregated with collagenase (1.5 mg/ml), and filtered through 70-μm strainers. Cells were stained with specific antibodies and Zombie Violet Fixable Viability Kit (BioLegend). Phenotype analysis was performed with the following antibodies purchased from BioLegend: anti-CD45–PerCp (peridinin chlorophyll protein) (30F11), anti-CD11b–APC (allophycocyanin) (M1/70), anti-CD3–PE (phycoerythrin)/Cy7 (17A2), anti-CD4–FITC (fluorescein isothiocyanate) (RM4-5), anti-CD8–PE or FITC (YTS156.7.7), anti-F4/80–APC (BM8), anti-CD49b–PE (DX5), anti-CD44–APC (IM7), anti-CD69–PE (H1.2F3), anti-CD62L–PE/Cy7 (MEL-14), anti-CD11c–FITC (N418), anti-CD28–PE (37.51), anti-CD25–APC (PC61), anti-CD127–PE/Cy7 (A7R34), and anti-FoxP3–PE (MF-14). For FoxP3 staining, cells were isolated and stained with surface antibodies for 30 min and then fixed and permeabilized using the FoxP3 Fix/Perm Buffer set (BioLegend). Cells were then stained with FoxP3-PE (BioLegend). For IFN-γ staining, cells were stimulated in vitro with the cell stimulation cocktail (eBioscience) and incubated with GolgiStop and GolgiPlug (BD Biosciences). After 6 hours of incubation, cells were washed and stained for extracellular markers. Then, cell permeabilization was performed by using the Cytofix/Cytoperm kit (BD Biosciences), and then the cells were stained for IFN-γ (XMG1.2, BioLegend). All flow cytometry was performed using the FACS Dako instrument and FlowJo software.

### Immunofluorescence analysis

Detection of T cells was performed with a modification of the method for immunofluorescence of fresh frozen tissues described previously (*32*). In brief, tumor samples were included in Killik (Bio-Optica), serially cut (10 μm), and fixed using cold acetone:methanol (1:1). Samples were incubated for 1 hour in blocking buffer [1% bovine serum albumin and 2% goat serum in phosphate-buffered saline (PBS) with 0.05% Tween and 0.1% Triton X-100] and incubated overnight with anti-CD8 (clone YTS169 from Thermo Fisher) and anti-CD4 (clone RM4-5 from Thermo Fisher). For detection, anti-rat Alexa Fluor 647 was used (Thermo Fisher Scientific). Nuclei were stained with 4′,6-diamidino-2-phenylindole (DAPI). Slides were then mounted using fluorescence mounting medium (Dako) and analyzed using a confocal laser scanning microscope (TCS SPE II; Leica).

### Plasma VitC analysis

The extraction procedure of ascorbic acid from plasma was carried out as previously reported (*50*), whereas the analytical part was developed on the basis of mass spectrometry technology, as recently reported (*22*, *23*). Heparinized plasma samples, previously supplemented with 10% of metaphosphoric acid, were defrosted, vortexed, and centrifuged at 13,200 rpm. Ninety-five microliters of the supernatant was supplemented with 5 μl of solution (190 μg/ml) of $^{13}C_6$-L-ascorbic acid as internal standard (IS), dissolved in acetonitrile:0.1% formic acid (70:30), then combined with 900 μl of acetonitrile:0.1% formic acid (70:30), and vortexed for 1 min. After centrifugation at 13,200 rpm for 10 min at 4°C, 200 μl was transferred to microvials and 5 μl was injected into liquid chromatography–tandem mass spectrometry (LC-MS/MS) instrumentation consisting of an LC

system Series 200 autosampler and micropump (Perkin Elmer) coupled to a triple quadrupole mass spectrometer API 4000 (SCIEX). Chromatographic separation was achieved on an Atlantis column T3 (2.1 mm × 150 mm, 3 μm) (Waters) fluxing mobile phase at a flow rate of 0.2 ml/min under gradient conditions. The mass spectrometer worked with electrospray ionization in negative ion mode and selected reaction monitoring, quantifying target ions mass/charge ratio ($m/z$) 175/115 for ascorbic acid and $m/z$ 181/119 for IS. The limit of quantification was 0.0055 mM; on the day of analysis, a plasma standard calibration curve was prepared in the range of 0.0055 to 5.7 mM. Samples with concentration above 5.7 mM were reanalyzed (diluted 1:1).

### Adoptive T cell transfer

Mice were euthanized, and their splenocytes were isolated as previously described (*28*). Briefly, spleens were minced and passed through a 70-μm cell strainer. Afterward, red blood cells were lysed with ACK lysis buffer (Gibco) and the remaining splenocytes were washed with magnetic-activated cell sorting (MACS) buffer. Magnetic bead sorting, using negative selection kit (Miltenyi), was used to acquire $CD4^+$ and $CD8^+$ T cells. The purity of the enriched cells was greater than 94%. Cells were dissolved in 100 μl of PBS and intravenously injected in an orthotopic model of breast cancer. Mice were injected twice with 5 million T cells by tail vein injection at days 5 and 10 since cancer cell injection.

### Antioxidant analysis

In experiments where antioxidants were administered, NAC was administered by oral gavage (1.2 g/kg in PBS, pH 7.2) as previously described (*51*–*53*). To check antioxidant effects on tumors, 8-oxoguanine (Abcam, N45.1) staining was performed by immunohistochemistry on formalin-fixed paraffin-embedded (FFPE) sections (*54*).

### Statistical analysis

Statistical analyses were performed using GraphPad Prism software. To determine statistical significance for tumor growth curves, normality and lognormality tests were performed for each experiment. In the case of a Gaussian-like distribution, Student's $t$ test for two-group comparison ($P$ values were adjusted with Welch correction) and one-way analysis of variance (ANOVA) for more than two-group comparison ($P$ values were adjusted with Tukey correction) were performed. In case of a non-Gaussian distribution, nonparametric tests were performed ($P$ values were adjusted with Welch correction). For immunophenotypic analysis, normality and lognormality tests were performed. Statistical significance was calculated using one-way ANOVA ($P$ values were adjusted with Tukey correction) in case of Gaussian-like distribution. Nonparametric analyses ($P$ values adjusted with Welch correction) were conducted for datasets that failed to pass a normality test. The Kaplan-Meier method was used for survival analysis, and $P$ values were calculated using the log-rank test (Mantel-Cox). All data are presented as mean ± SEM. Sample sizes were chosen to provide adequate power on the basis of our previous studies and literature surveys. The number of replicates and sample size for in vivo experiments were limited according to the requirements of the Italian Ministry of Health. Animal studies were performed in accordance with institutional guidelines and international law and policies. When therapy was applied, we performed randomization. In this case, only mice bearing tumors with a volume within 50% of the average size were included in the experiment. Original data are provided in data files S1 to S10.

## SUPPLEMENTARY MATERIALS

stm.sciencemag.org/cgi/content/full/12/532/eaay8707/DC1

Fig. S1. VitC quantification in plasma.
Fig. S2. High doses of VitC are required for maximal antiproliferative effects in murine breast tumors.
Fig. S3. Administration of antioxidant NAC does not impair VitC anticancer effect.
Fig. S4. Flow cytometry for IFN-γ in spleen-derived T lymphocytes.
Fig. S5. Isolation of T cells for adoptive T cell transfer.
Fig. S6. Depletion of CD4 T cells for adoptive cell transfer experiments.
Fig. S7. Tumor growth of individual mice treated as shown in Fig. 3 (A and B).
Fig. S8. Tumor growth of individual mice treated as shown in Fig. 3 (C to E).
Fig. S9. Modulation of tumor immune infiltration induced by VitC.
Fig. S10. Flow cytometry on CD44 and CD69 T cell markers on CD4 T lymphocytes.
Fig. S11. Representative CD44- and CD69-positive events on CD8 T lymphocytes by flow cytometry.
Fig. S12. VitC effect on growth of MMR-deficient tumors in NOD-SCID mice.
Fig. S13. Tumor growth of individual mice bearing MLH1-KO tumors and treated with ICT and VitC as shown in Fig. 5D.
Fig. S14. Tumor volume variations since treatment start of TS/A MLH1-KO and CT26 MLH1-KO tumors treated with ICT and VitC.
Data file S1. Tumor measurements of experiments in Fig. 1.
Data file S2. Tumor measurements of experiments in Fig. 2.
Data file S3. Tumor measurements of experiments in Fig. 3.
Data file S4. Immuno-phenotiping of CD4 and CD8 T cells.
Data file S5. Tumor measurements of experiments in Fig. 5.
Data file S6. Plasma VitC analysis.
Data file S7. Tumor measurements of experiments in figs. S2 and S3.
Data file S8. Tumor measurements of experiments in fig. S6.
Data file S9. Tumor measurements of experiments in fig. S8.
Data file S10. Tumor measurements of experiments in fig. S12.

View/request a protocol for this paper from *Bio-protocol*.

## REFERENCES AND NOTES


1. L. A. Diaz, D. T. Le, PD-1 blockade in tumors with mismatch-repair deficiency. *N. Engl. J. Med.* **373**, 1979 (2015).
2. D. T. Le, J. N. Durham, K. N. Smith, H. Wang, B. R. Bartlett, L. K. Aulakh, S. Lu, H. Kemberling, C. Wilt, B. S. Luber, F. Wong, N. S. Azad, A. A. Rucki, D. Laheru, R. Donehower, A. Zaheer, G. A. Fisher, T. S. Crocenzi, J. J. Lee, T. F. Greten, A. G. Duffy, K. K. Ciombor, A. D. Eyring, B. H. Lam, A. Joe, S. P. Kang, M. Holdhoff, L. Danilova, L. Cope, C. Meyer, S. Zhou, R. M. Goldberg, D. K. Armstrong, K. M. Bever, A. N. Fader, J. Taube, F. Housseau, D. Spetzler, N. Xiao, D. M. Pardoll, N. Papadopoulos, K. W. Kinzler, J. R. Eshleman, B. Vogelstein, R. A. Anders, L. A. Diaz Jr., Mismatch repair deficiency predicts response of solid tumors to PD-1 blockade. *Science* **357**, 409–413 (2017).
3. M. K. Callahan, H. Kluger, M. A. Postow, N. H. Segal, A. Lesokhin, M. B. Atkins, J. M. Kirkwood, S. Krishnan, R. Bhore, C. Horak, J. D. Wolchok, M. Sznol, Nivolumab plus ipilimumab in patients with advanced melanoma: Updated survival, response, and safety data in a phase I dose-escalation study. *J. Clin. Oncol.* **36**, 391–398 (2018).
4. N. A. Rizvi, M. D. Hellmann, A. Snyder, P. Kvistborg, V. Makarov, J. J. Havel, W. Lee, J. Yuan, P. Wong, T. S. Ho, M. L. Miller, N. Rekhtman, A. L. Moreira, F. Ibrahim, C. Bruggeman, B. Gasmi, R. Zappasodi, Y. Maeda, C. Sander, E. B. Garon, T. Merghoub, J. D. Wolchok, T. N. Schumacher, T. A. Chan, Mutational landscape determines sensitivity to PD-1 blockade in non-small cell lung cancer. *Science* **348**, 124–128 (2015).
5. M. D. Hellmann, T.-E. Ciuleanu, A. Pluzanski, J. S. Lee, G. A. Otterson, C. Audigier-Valette, E. Minenza, H. Linardou, S. Burgers, P. Salman, H. Borghaei, S. S. Ramalingam, J. Brahmer, M. Reck, K. J. O'Byrne, W. J. Geese, G. Green, H. Chang, J. Szustakowski, P. Bhagavatheeswaran, D. Healey, Y. Fu, F. Nathan, L. Paz-Ares, Nivolumab plus ipilimumab in lung cancer with a high tumor mutational burden. *N. Engl. J. Med.* **378**, 2093–2104 (2018).
6. J. Bellmunt, R. de Wit, D. J. Vaughn, Y. Fradet, J. L. Lee, L. Fong, N. J. Vogelzang, M. A. Climent, D. P. Petrylak, T. K. Choueiri, A. Necchi, W. Gerritsen, H. Gurney, D. I. Quinn, S. Culine, C. N. Sternberg, Y. Mai, C. H. Poehlein, R. F. Perini, D. F. Bajorin; KEYNOTE-045 Investigators, Pembrolizumab as second-line therapy for advanced urothelial carcinoma. *N. Engl. J. Med.* **376**, 1015–1026 (2017).
7. M. J. Overman, S. Lonardi, K. Y. M. Wong, H.-J. Lenz, F. Gelsomino, M. Aglietta, M. A. Morse, E. van Cutsem, R. McDermott, A. Hill, M. B. Sawyer, A. Hendlisz, B. Neyns, M. Svrcek, R. A. Moss, J.-M. Ledeine, Z. A. Cao, S. Kamble, S. Kopetz, T. André, Durable clinical benefit with nivolumab plus ipilimumab in DNA mismatch repair-deficient/microsatellite instability-high metastatic colorectal cancer. *J. Clin. Oncol.* **36**, 773–779 (2018).

8. M. J. Overman, R. McDermott, J. L. Leach, S. Lonardi, H. J. Lenz, M. A. Morse, J. Desai, A. Hill, M. Axelson, R. A. Moss, M. V. Goldberg, Z. A. Cao, J. M. Ledeine, G. A. Maglinte, S. Kopetz, T. André, Nivolumab in patients with metastatic DNA mismatch repair-deficient or microsatellite instability-high colorectal cancer (CheckMate 142): An open-label, multicentre, phase 2 study. *Lancet Oncol.* **18**, 1182–1191 (2017).
9. S. Adams, P. Schmid, H. S. Rugo, E. P. Winer, D. Loirat, A. Awada, D. W. Cescon, H. Iwata, M. Campone, R. Nanda, R. Hui, G. Curigliano, D. Toppmeyer, J. O'Shaughnessy, S. Loi, S. Paluch-Shimon, A. R. Tan, D. Card, J. Zhao, V. Karantza, J. Cortés, Pembrolizumab monotherapy for previously treated metastatic triple-negative breast cancer: Cohort a of the phase II KEYNOTE-086 study. *Ann. Oncol.* **30**, 397–404 (2019).
10. J. Gong, A. Hendifar, R. Tuli, J. Chuang, M. Cho, V. Chung, D. Li, R. Salgia, Combination systemic therapies with immune checkpoint inhibitors in pancreatic cancer: Overcoming resistance to single-agent checkpoint blockade. *Clin. Transl. Med.* **7**, 32 (2018).
11. D. T. Le, J. N. Uram, H. Wang, B. R. Bartlett, H. Kemberling, A. D. Eyring, A. D. Skora, B. S. Luber, N. S. Azad, D. Laheru, B. Biedrzycki, R. C. Donehower, A. Zaheer, G. A. Fisher, T. S. Crocenzi, J. J. Lee, S. M. Duffy, R. M. Goldberg, A. de la Chapelle, M. Koshiji, F. Bhaijee, T. Huebner, R. H. Hruban, L. D. Wood, N. Cuka, D. M. Pardoll, N. Papadopoulos, K. W. Kinzler, S. Zhou, T. C. Cornish, J. M. Taube, R. A. Anders, J. R. Eshleman, B. Vogelstein, L. A. Diaz Jr., PD-1 blockade in tumors with mismatch-repair deficiency. *N. Engl. J. Med.* **372**, 2509–2520 (2015).
12. S. J. Padayatty, M. Levine, Vitamin C: The known and the unknown and goldilocks. *Oral Dis.* **22**, 463–493 (2016).
13. A. C. Carr, S. Maggini, Vitamin C and immune function. *Nutrients* **9**, E1211 (2017).
14. A. Sorice, E. Guerriero, F. Capone, G. Colonna, G. Castello, S. Costantini, Ascorbic acid: Its role in immune system and chronic inflammation diseases. *Mini Rev. Med. Chem.* **14**, 444–452 (2014).
15. X. Yue, S. Trifari, T. Äijö, A. Tsagaratou, W. A. Pastor, J. A. Zepeda-Martínez, C. W. J. Lio, X. Li, Y. Huang, P. Vijayanand, H. Lähdesmäki, A. Rao, Control of Foxp3 stability through modulation of TET activity. *J. Exp. Med.* **213**, 377–397 (2016).
16. M. Agathocleous, C. E. Meacham, R. J. Burgess, E. Piskounova, Z. Zhao, G. M. Crane, B. L. Cowin, E. Bruner, M. M. Murphy, W. Chen, G. J. Spangrude, Z. Hu, R. J. DeBerardinis, S. J. Morrison, Ascorbate regulates haematopoietic stem cell function and leukaemogenesis. *Nature* **549**, 476–481 (2017).
17. J. Manning, B. Mitchell, D. A. Appadurai, A. Shakya, L. J. Pierce, H. Wang, V. Nganga, P. C. Swanson, J. M. May, D. Tantin, G. J. Spangrude, Vitamin C promotes maturation of T-cells. *Antioxid. Redox Signal.* **19**, 2054–2067 (2013).
18. K. Blaschke, K. T. Ebata, M. M. Karimi, J. A. Zepeda-Martínez, P. Goyal, S. Mahapatra, A. Tam, D. J. Laird, M. Hirst, A. Rao, M. C. Lorincz, M. Ramalho-Santos, Vitamin C induces Tet-dependent DNA demethylation and a blastocyst-like state in ES cells. *Nature* **500**, 222–226 (2013).
19. E. Cameron, L. Pauling, Supplemental ascorbate in the supportive treatment of cancer: Prolongation of survival times in terminal human cancer. *Proc. Natl. Acad. Sci. U.S.A.* **73**, 3685–3689 (1976).
20. C. G. Moertel, T. R. Fleming, E. T. Creagan, J. Rubin, M. J. O'Connell, M. M. Ames, High-dose vitamin C versus placebo in the treatment of patients with advanced cancer who have had no prior chemotherapy—A randomized double-blind comparison. *N. Engl. J. Med.* **312**, 137–141 (1985).
21. S. J. Padayatty, H. Sun, Y. Wang, H. D. Riordan, S. M. Hewitt, A. Katz, R. A. Wesley, M. Levine, Vitamin C pharmacokinetics: Implications for oral and intravenous use. *Ann. Intern. Med.* **140**, 533–537 (2004).
22. J. D. Schoenfeld, Z. A. Sibenaller, K. A. Mapuskar, B. A. Wagner, K. L. Cramer-Morales, M. Furqan, S. Sandhu, T. L. Carlisle, M. C. Smith, T. Abu Hejleh, D. J. Berg, J. Zhang, J. Keech, K. R. Parekh, S. Bhatia, V. Monga, K. L. Bodeker, L. Ahmann, S. Vollstedt, H. Brown, E. P. S. Kauffman, M. E. Schall, R. J. Hohl, G. H. Clamon, J. D. Greenlee, M. A. Howard, M. K. Schultz, B. J. Smith, D. P. Riley, F. E. Domann, J. J. Cullen, G. R. Buettner, J. M. Buatti, D. R. Spitz, B. G. Allen, $O_2^{\cdot-}$ and $H_2O_2$-mediated disruption of Fe metabolism causes the differential susceptibility of NSCLC and GBM cancer cells to pharmacological ascorbate. *Cancer Cell* **32**, 268 (2017).
23. J. Yun, E. Mullarky, C. Lu, K. N. Bosch, A. Kavalier, K. Rivera, J. Roper, I. I. C. Chio, E. G. Giannopoulou, C. Rago, A. Muley, J. M. Asara, J. Paik, O. Elemento, Z. Chen, D. J. Pappin, L. E. Dow, N. Papadopoulos, S. S. Gross, L. C. Cantley, Vitamin C selectively kills *KRAS* and *BRAF* mutant colorectal cancer cells by targeting *GAPDH*. *Science* **350**, 1391–1396 (2015).
24. B. Ngo, J. M. Van Riper, L. C. Cantley, J. Yun, Targeting cancer vulnerabilities with high-dose vitamin C. *Nat. Rev. Cancer* **19**, 271–282 (2019).
25. N. Shenoy, E. Creagan, T. Witzig, M. Levine, Ascorbic acid in cancer treatment: Let the phoenix fly. *Cancer Cell* **34**, 700–706 (2018).
26. A. C. Carr, J. Cook, Intravenous vitamin C for cancer therapy - identifying the current gaps in our knowledge. *Front. Physiol.* **9**, 1182 (2018).
27. S. C. Wei, C. R. Duffy, J. P. Allison, Fundamental mechanisms of immune checkpoint blockade therapy. *Cancer Discov.* **8**, 1069–1086 (2018).
28. N. G. Kooreman, Y. Kim, P. E. de Almeida, V. Termglinchan, S. Diecke, N. Y. Shao, T. T. Wei, H. Yi, D. Dey, R. Nelakanti, T. P. Brouwer, D. T. Paik, I. Sagiv-Barfi, A. Han, P. H. A. Quax, J. F. Hamming, R. Levy, M. M. Davis, J. C. Wu, Autologous iPSC-based vaccines elicit anti-tumor responses in vivo. *Cell Stem Cell* **22**, 501–513.e7 (2018).
29. Y.-J. Park, D.-S. Kuen, Y. Chung, Future prospects of immune checkpoint blockade in cancer: From response prediction to overcoming resistance. *Exp. Mol. Med.* **50**, 109 (2018).
30. P. Darvin, S. M. Toor, V. Sasidharan Nair, E. Elkord, Immune checkpoint inhibitors: Recent progress and potential biomarkers. *Exp. Mol. Med.* **50**, 165 (2018).
31. K. Kim, A. D. Skora, Z. Li, Q. Liu, A. J. Tam, R. L. Blosser, L. A. Diaz Jr., N. Papadopoulos, K. W. Kinzler, B. Vogelstein, S. Zhou, Eradication of metastatic mouse cancers resistant to immune checkpoint blockade by suppression of myeloid-derived cells. *Proc. Natl. Acad. Sci. U.S.A.* **111**, 11774–11779 (2014).
32. G. Germano, S. Lamba, G. Rospo, L. Barault, A. Magrì, F. Maione, M. Russo, G. Crisafulli, A. Bartolini, G. Lerda, G. Siravegna, B. Mussolin, R. Frapolli, M. Montone, F. Morano, F. de Braud, N. Amirouchene-Angelozzi, S. Marsoni, M. D'Incalci, A. Orlandi, E. Giraudo, A. Sartore-Bianchi, S. Siena, F. Pietrantonio, F. di Nicolantonio, A. Bardelli, Inactivation of DNA repair triggers neoantigen generation and impairs tumour growth. *Nature* **552**, 116–120 (2017).
33. J. Liu, S. J. Blake, H. Harjunpää, K. A. Fairfax, M. C. R. Yong, S. Allen, H. E. Kohrt, K. Takeda, M. J. Smyth, M. W. L. Teng, Assessing immune-related adverse events of efficacious combination immunotherapies in preclinical models of cancer. *Cancer Res.* **76**, 5288–5301 (2016).
34. E. J. Campbell, M. C. M. Vissers, C. Wohlrab, K. O. Hicks, R. M. Strother, S. M. Bozonet, B. A. Robinson, G. U. Dachs, Pharmacokinetic and anti-cancer properties of high dose ascorbate in solid tumours of ascorbate-dependent mice. *Free Radic. Biol. Med.* **99**, 451–462 (2016).
35. Y. P. Xu, L. Lv, Y. Liu, M. D. Smith, W. C. Li, X. M. Tan, M. Cheng, Z. Li, M. Bovino, J. Aubé, Y. Xiong, Tumor suppressor TET2 promotes cancer immunity and immunotherapy efficacy. *J. Clin. Invest.* **130**, 4316–4331 (2019).
36. O. K. Serrano, N. L. Parrow, P. C. Violet, J. Yang, J. Zornjak, A. Basseville, M. Levine, Antitumor effect of pharmacologic ascorbate in the B16 murine melanoma model. *Free Radic. Biol. Med.* **87**, 193–203 (2015).
37. V. Sasidharan Nair, M. H. Song, K. I. Oh, Vitamin C facilitates demethylation of the *Foxp3* enhancer in a Tet-dependent manner. *J. Immunol.* **196**, 2119–2131 (2016).
38. Y. J. Jeong, J. H. Kim, J. M. Hong, J. S. Kang, H. R. Kim, W. J. Lee, Y. I. Hwang, Vitamin C treatment of mouse bone marrow-derived dendritic cells enhanced $CD8^+$ memory T cell production capacity of these cells in vivo. *Immunobiology* **219**, 554–564 (2014).
39. J. I. Young, S. Züchner, G. Wang, Regulation of the epigenome by vitamin C. *Annu. Rev. Nutr.* **35**, 545–564 (2015).
40. H. E. Ghoneim, Y. Fan, A. Moustaki, H. A. Abdelsamed, P. Dash, P. Dogra, R. Carter, W. Awad, G. Neale, P. G. Thomas, B. Youngblood, De novo epigenetic programs inhibit PD-1 blockade-mediated T cell rejuvenation. *Cell* **170**, 142–157.e19 (2017).
41. P. Arnaud-Coffin, D. Maillet, H. K. Gan, J.-J. Stelmes, B. You, S. Dalle, J. Péron, A systematic review of adverse events in randomized trials assessing immune checkpoint inhibitors. *Int. J. Cancer* **145**, 639–648 (2019).
42. R. A. Luchtel, T. Bhagat, K. Pradhan, W. R. Jacobs Jr., M. Levine, A. Verma, N. Shenoy, High-dose ascorbic acid synergizes with anti-PD1 in a lymphoma mouse model. *Proc. Natl. Acad. Sci. U.S.A.* **117**, 1666–1677 (2020).
43. F. Wang, M.-M. He, Z.-X. Wang, S. Li, Y. Jin, C. Ren, S.-M. Shi, B.-T. Bi, S.-Z. Chen, Z.-D. Lv, J.-J. Hu, Z.-Q. Wang, F.-H. Wang, D.-S. Wang, Y.-H. Li, R.-H. Xu, Phase I study of high-dose ascorbic acid with mFOLFOX6 or FOLFIRI in patients with metastatic colorectal cancer or gastric cancer. *BMC Cancer* **19**, 460 (2019).
44. A. C. Carr, C. McCall, The role of vitamin C in the treatment of pain: New insights. *J. Transl. Med.* **15**, 77 (2017).
45. P. Nanni, C. de Giovanni, P. L. Lollini, G. Nicoletti, G. Prodi, TS/a: A new metastasizing cell line from a BALB/c spontaneous mammary adenocarcinoma. *Clin. Exp. Metastasis* **1**, 373–380 (1983).
46. T. H. Corbett, D. P. Griswold Jr., B. J. Roberts, J. C. Peckham, F. M. Schabel, Tumor induction relationships in development of transplantable cancers of the colon in mice for chemotherapy assays, with a note on carcinogen structure. *Cancer Res.* **35**, 2434–2439 (1975).
47. D. L. Dexter, H. M. Kowalski, B. A. Blazar, Z. Fligiel, R. Vogel, G. H. Heppner, Heterogeneity of tumor cells from a single mouse mammary tumor. *Cancer Res.* **38**, 3174–3181 (1978).
48. M. E. Gilles, F. Maione, M. Cossutta, G. Carpentier, L. Caruana, S. di Maria, C. Houppe, D. Destouches, K. Shchors, C. Prochasson, F. Mongelard, S. Lamba, A. Bardelli, P. Bouvet, A. Couvelard, J. Courty, E. Giraudo, I. Cascone, Nucleolin targeting impairs the progression of pancreatic cancer and promotes the normalization of tumor vasculature. *Cancer Res.* **76**, 7181–7193 (2016).
49. I. J. Fidler, Selection of successive tumour lines for metastasis. *Nat. New Biol.* **242**, 148–149 (1973).
50. A. Karlsen, R. Blomhoff, T. E. Gundersen, Stability of whole blood and plasma ascorbic acid. *Eur. J. Clin. Nutr.* **61**, 1233–1236 (2007).

51. D. Arfsten, E. W. Johnson, A. R. Thitoff, A. E. Jung, E. R. Wilfong, S. M. Lohrke, T. A. Bausman, J. S. Eggers, A. J. Bobb, Impact of 30-day oral dosing with *N*-acetyl-L-cysteine on Sprague-Dawley rat physiology. *Int. J. Toxicol.* **23**, 239–247 (2016).
52. A. E. Kane, A. Huizer-Pajkos, J. Mach, C. McKenzie, S. J. Mitchell, R. de Cabo, B. Jones, V. Cogger, D. G. le Couteur, S. N. Hilmer, *N*-acetyl cysteine does not prevent liver toxicity from chronic low-dose plus subacute high-dose paracetamol exposure in young or old mice. *Fundam. Clin. Pharmacol.* **30**, 263–275 (2016).
53. B. H. Harvey, C. Joubert, J. L. du Preez, M. Berk, Effect of chronic N-acetyl cysteine administration on oxidative status in the presence and absence of induced oxidative stress in rat striatum. *Neurochem. Res.* **33**, 508–517 (2008).
54. V. I. Sayin, M. X. Ibrahim, E. Larsson, J. A. Nilsson, P. Lindahl, M. O. Bergo, Antioxidants accelerate lung cancer progression in mice. *Sci Transl. Med.* **6**, 221ra15 (2014).

**Acknowledgments:** We thank members of the Molecular Oncology laboratory at IRCCS Candiolo Cancer Institute for critically reading the manuscript. We also thank L. Pace for insightful scientific discussion and S. Giove for help with immunohistochemistry experiments. **Funding:** This research was funded by FONDAZIONE AIRC under 5 per Mille 2018 (ID 21091 program; principal investigator, A.B.; group leader, F.D.N.; group leader, S.A.), AIRC IG 2018 (ID 21923 project; principal investigator, A.B.), AIRC-CRUK-FC AECC Accelerator Award contract 22795 (A.B.), and AIRC IG 2018 (ID 21407 project; principal investigator, F.D.N.). This work was also funded by European Community's Seventh Framework Programme GA n. 602901 MErCuRIC (A.B.), European Community's Horizon 2020 GA n. 635342-2 MoTriColor (A.B.), IMI contract n. 115749 CANCER-ID (A.B.), Fondazione Piemontese per la Ricerca sul Cancro-ONLUS 5 per mille 2014 e 2015 Ministero della Salute Project "STRATEGY" (F.D.N.), Project "IMMUNOGENOMICA" (A.B.), and Progetto NET-2011-02352137 Ministero della Salute. **Author contributions:** A.B., F.D.N., and A.M. conceived the study. A.M., R.C., M.M., and V.A. performed animal experiments. A.M., G.G., A.L., and F.S. performed immunophenotypic and immunohistochemistry analysis. S.L. generated mouse cell models. M.D., M.Z., and T.C. performed plasma VitC quantification. A.B., F.D.N., A.M., and G.G. interpreted the data. S. Abrignani and S. Arena assisted in critical discussion of the data. A.B., F.D.N., and A.M. wrote the manuscript. A.B. and F.D.N. supervised the study. **Competing interests:** A.B has served as an advisor for Biocartis, Guardant, Boehringer, and Roche. A.B. is a member of the scientific advisory board of NeoPhore and Horizon Discovery. A.B. and G.G. are shareholder of NeoPhore. The other authors declare that they have no competing interests. **Data and materials availability:** The *MLH1* knockout cells are available from A.B. and G.G. under a material transfer agreement with the University of Torino.

Submitted 30 July 2019
Resubmitted 23 December 2019
Accepted 3 February 2020
Published 26 February 2020
10.1126/scitranslmed.aay8707

**Citation:** A. Magrì, G. Germano, A. Lorenzato, S. Lamba, R. Chilà, M. Montone, V. Amodio, T. Ceruti, F. Sassi, S. Arena, S. Abrignani, M. D'Incalci, M. Zucchetti, F. Di Nicolantonio, A. Bardelli, High-dose vitamin C enhances cancer immunotherapy. *Sci. Transl. Med.* **12**, eaay8707 (2020).

Science Translational Medicine

# High-dose vitamin C enhances cancer immunotherapy

Alessandro Magrì, Giovanni Germano, Annalisa Lorenzato, Simona Lamba, Rosaria Chilà, Monica Montone, Vito Amodio, Tommaso Ceruti, Francesco Sassi, Sabrina Arena, Sergio Abrignani, Maurizio D'Incalci, Massimo Zucchetti, Federica Di Nicolantonio and Alberto Bardelli

*Sci Transl Med* **12**, eaay8707.
DOI: 10.1126/scitranslmed.aay8707

**A vitamin boost for immunotherapy**

Despite some controversy over the years, it is gradually becoming clear that vitamin C has some anticancer effects, albeit only when given intravenously and at sufficiently high doses. However, earlier studies evaluating the anticancer effects of vitamin C have used immunodeficient mice and therefore only examined its direct effects on tumors. By studying immunocompetent mouse models of cancer, Magri *et al.* determined that the vitamin's effects were much stronger in the presence of an intact immune system and that it cooperated with checkpoint immunotherapy. These findings suggest a promising approach to combination treatment, which now needs to be tested in patients.